

# Systematic Study of Hadronic Observables in Nucleus Nucleus Collisions at CERN SPS

R. Ganz<sup>1</sup> for the NA49 collaboration

<sup>1</sup> Max-Planck-Institut für Physik München, Föhringer Ring 6, D-80805 München, Germany

e-mail: Rudolf.Ganz@cern.ch

## Abstract

The possible transition of nuclear matter to a deconfined phase in relativistic nucleus-nucleus collisions is explored by a systematic variation of the collision system by means of system size, beam energy and centrality of the collision all measured within the same experiment NA49 at the CERN SPS. The investigation takes advantage of the large number of hadronic observables covered over a wide phase space by the acceptance of the NA49 TPCs.

## 1. Introduction

The aim of studying nucleus-nucleus collisions at relativistic beam energies is the potential creation of a new state of matter, the Quark Gluon Plasma, in which quarks are no longer confined to a single nucleon but can move quasi-freely over a larger volume. The highly dense environment, an essential for the occurrence of this state, might be established for a short period of time in collisions of two heavy nuclei at relativistic beam energies at the CERN SPS. Because so far no signature has been put forward, which would uniquely identify the transition to such a state simply by its mere observation, only a systematic study can reveal the onset of such a new phenomenon. The NA49 collaboration at CERN SPS has undertaken such a systematic approach by a variation of the initial state of the collision in terms of collision systems (p+p, p+Pb and Pb+Pb), different centralities and two beam energies (40 AGeV and 158 AGeV). Due to the versatility of NA49[1] in all these systems a large number of observables has been surveyed over wide phase space (see [2] and ref. therein), all within the same experimental setup. Here we present only a few aspects focussing on identified charged particle spectra and two particle correlations.

## 2. Identified particle spectra

In NA49 two methods of identifying particles are utilized. The more stringent method utilizes a time-of-flight measurement by four scintillator walls over

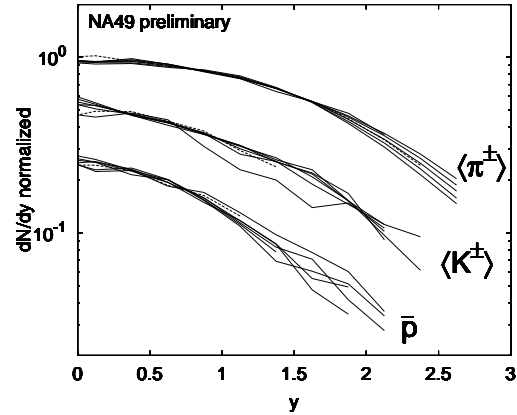


**Figure 1.** Shape of the rapidity distribution of average charged pions, kaons and anti-protons. The results are from p+p collisions (dashed line) and Pb+Pb collision (solid lines) in six bins of centrality and are normalized at  $y = 0$ .

a flight-path of 13 m. Since in this case the coverage of phase space is rather limited the results presented here are based on the second method, which exploits the specific energy loss  $dE/dx$  (resolution typically 4%) deposited by charged particles in the gas of the four large volume time projections chambers of NA49[1].

Figure 1 shows a comparison of the shapes of the rapidity distributions for pions ( $\langle \pi^+ + \pi^- \rangle / 2$ ), kaons ( $\langle K^+ + K^- \rangle / 2$ ), and anti-protons

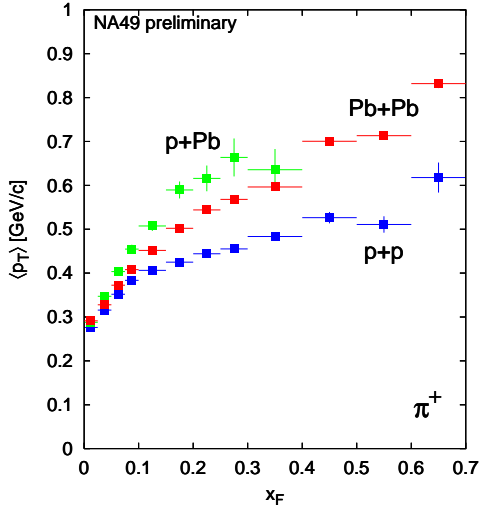


**Figure 2.** Average transverse momentum in dependence on Feynman- $x$   $x_F$  for  $\pi^+$  in p+p, central p+Pb and central Pb+Pb collisions.

measured in p+p collisions as well as in Pb+Pb collisions at six different bins of centrality (average impact parameters  $\langle b \rangle \approx 2.6, 4.6, 5.7, 7.0, 8.5$  and  $10.5$  fm) all at the incident beam energy of  $158$  AGeV. It appears that the shapes are almost identical over this large variety of collision systems even though the change in system volume and geometry is rather sizeable.

Turning attention to the transverse momentum distribution, the first question one might ask is, whether it is independent from the longitudinal component. This is addressed in figures 2 and 3 by plotting the average transverse momentum  $\langle p_T \rangle$  versus the longitudinal momentum component, the latter being represented by the x-Feynman  $x_F$  variable. For pions the seagull-shaped wing of figure 2 contradicts the independence of the two $\ddagger$ . This might be due to the contribution of low- $p_T$  pions from resonance decays at mid-rapidity, whereas a direct production rules at more forward rapidities.

For proton spectra the situation is changed. Here, with the exception of the asymmetric projectile-target system p+Pb, the assumption of an independence between longitudinal and transverse momentum is well supported by an almost constant  $\langle p_T \rangle$  value for regions of rapidities (figure 3). To interpret this one should keep in mind that in this energy regime the proton yield is still

$\ddagger$  A fact not to be neglected when extrapolating results from narrow acceptance experiments into full phase space.

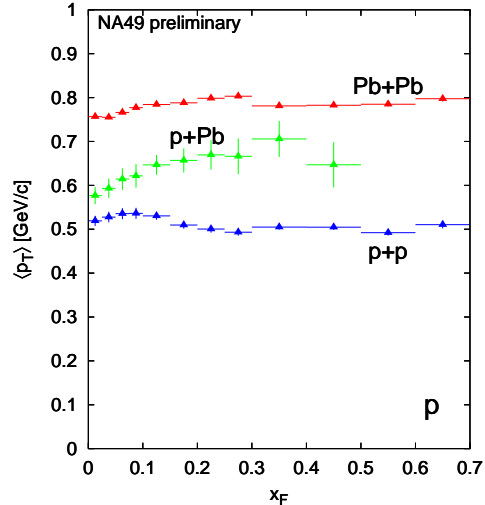


**Figure 3.** Same representation as previous figure but shown for protons instead.

dominated by the number of incoming projectile and target nucleons. The overall increase in  $\langle p_T \rangle$  from p+p to Pb+Pb might be attributed to the increased transfer of longitudinal momentum into transversal degrees of freedom due to multiple collisions.

### 3. Two particle correlations

Two particle correlations, here by means of the quantum mechanical interference of two identical pions, offer the opportunity to study the space-time evolution of heavy ion collisions in a direct way. With respect to the observation of a deconfined phase, this might be important since a transition should be accompanied by an increase in entropy, which in the final state of the collision should emerge as an increase in overall multiplicity or/and as an increase in the systems space-time extent compared to the case when no such transition has occurred.

In the right column of figure 4 the dependence of the fitted radius parameters on the number  $n_{\text{part}}$  of nucleons participating in the collision is shown for Pb+Pb collisions at different centralities compared to NA49 results from p+p reactions and to the NA35 results [5] on S+S at  $200$  AGeV. The transverse radii  $R_{\text{side}}$  and  $R_{\text{out}}$  grow continuously whereas  $R_{\text{long}}$  appears constant when increasing  $n_{\text{part}}$ .  $R_{\text{diff}}^2 = R_{\text{out}}^2 - R_{\text{side}}^2$ , being sensitive to the duration of the particle emission phase, is positive over the full range and  $R_{\text{diff}}$  grows linearly with

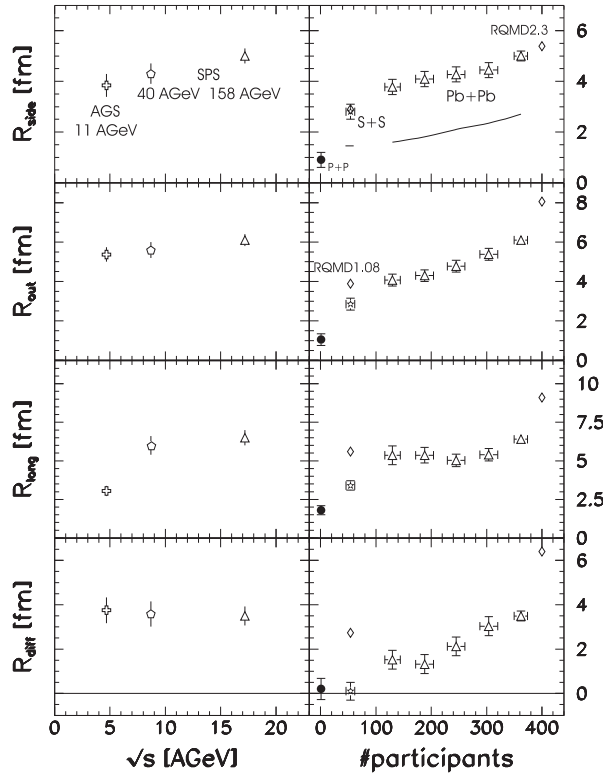


**Figure 4.** *Left column:* Dependence of radii on the center of mass energy. The 4.7 AGeV points are AGS Au+Au data from E866 [6]. The 8.7 AGeV radii are our very preliminary 40 AGeV Pb+Pb results and the 17.2 AGeV points are for central 158 AGeV Pb+Pb. *Right column:* Dependence of the radii on number of participants in the collision. The  $\Delta$  correspond to different centralities in 158 AGeV Pb+Pb. Symbol  $\star$  is for central 200 AGeV S+S [5] and  $\bullet$  is for the 158 AGeV p+p result. The  $\diamond$  is the RQMD 1.08 result for central S+S and the RQMD 2.3 result for central Pb+Pb. The line in  $R_{\text{side}}$  corresponds to the geometrical transverse size of the overlap region of the two colliding nuclei. ( $\langle y_{\pi\pi} \rangle \approx 4.2$  and  $\langle k_t \rangle \approx 0.12$  GeV/c .)

$n_{\text{part}}$ . When comparing the measured radii with those extracted from the RQMD model, similar to the findings of NA35, a good agreement is found for  $R_{\text{side}}$ , but both versions of the model overestimate  $R_{\text{out}}$  and  $R_{\text{long}}$ . It is instructive to compare  $R_{\text{side}}$  with an estimate of the geometrical transverse size of the overlap region in the collisions (line§ in figure 4) which demonstrates that the

§ The line in  $R_{\text{side}}$  corresponds to the average distance of points in the overlap region of two spheres of radius  $1.16A^{1/3}$  offset by the impact parameter from the center of the collision, projected into a randomly oriented reaction plane.

interferometric radii reflect the late freeze-out stage which is preceded by a strong expansion of the dense collision zone produced shortly after the collision [4]. The left column of figure 4 shows the collision energy dependence of the radius parameters displaying results for the highest AGS energy at 11.6 AGeV, the SPS measurements at 158 AGeV and the (very preliminary) results from the 40 AGeV commissioning run of NA49 in 1998. The 40 AGeV and the 158 AGeV results correspond to  $\frac{\langle y_{\pi\pi} \rangle - y_{\text{cms}}}{y_{\text{cms}}} \approx 1.0$  whereas the AGS measurement [6] covers mid-rapidity. The comparison is justified by the observed slow variation of the radii with  $y_{\pi\pi}$  in NA49. From AGS to the highest SPS energy  $R_{\text{long}}$  more than doubles whereas the transverse radii  $R_{\text{out}}$  and  $R_{\text{side}}$  and the derived temporal component  $R_{\text{diff}}$  stay almost constant.

#### 4. Summary

A systematic study of hadronic observables in heavy ion collisions has been carried out by the NA49 experiment. In none of the discussed variables a sudden change has been observed, which would indicate a sharp QGP phase transition. In particular the longitudinal shapes of the produced particle spectra seem to be unchanged coming from p+p moving towards the most central Pb+Pb collisions. The interferometric radii follow smooth trends when increasing centrality, when changing the collision system or (with the exception of  $R_{\text{long}}$ ) when increasing the incident beam energy from the AGS to SPS.

#### References

- [1] S. Afanasiev et al., NIM A430(1999)210.
- [2] F. Sikler et al., in proc. of Quark Matter 99, Torino It., to be publ. in Nucl. Phys.A
- [3] R. Ganz et al., in proc. of Quark Matter 99, Torino It., to be publ. in Nucl. Phys.A
- [4] H. Appelshäuser et al., Euro. Phys. Jour. C2(1998) 611.
- [5] T. Alber et al., Phys. Rev. Lett. 74(1995) 1303 and Nucl. Phys. A590(1995) 453.
- [6] R. Soltz for E866, in proc. of Quark Matter 99, Torino It., to be publ. in Nucl. Phys.A